Electrochemistry

Received: July 26, 2014
Accepted: November 20, 2014
Published: February 5, 2015

The Electrochemical Society of Japan

http://dx.doi.org/10.5796/electrochemistry.83.76

Article

Electrochemistry, **83(2)**, 76–79 (2015)

Effect of Sputtering Power on the Electrochemical Properties of Low Loaded Pt Catalysts for PEM Fuel Cell

Oguz Kaan OZDEMIR[a,b,*]

[a] *Department of Metallurgical and Material Engineering, Yildiz Tech. University, Istanbul, Turkey*
[b] *Nanotechnology Research Center, Gebze Institute of Technology, Kocaeli, Turkey*

* *Corresponding author: kozdemir@yildiz.edu.tr*

ABSTRACT

A series of thin Pt films were deposited by dc magnetron sputtering with different power directly on a commercial hydrophobic carbon paper substrate at room temperature. Their electrochemical properties toward the oxygen reduction reaction were investigated in 0.5 M H_2SO_4 solution by means of cyclic voltametry (CV) and linear sweep voltametry (LSV) on rotating disc electrode (RDE). It was found that the increase of power leads to rise in the electrochemical active surface area (*EASA*) slightly up to 25 W, but further increase in power decreases surface area significantly. Electrochemical surface area is reaching a maximum of 29.68 $m^2 g_{Pt}^{-1}$ for 25 W. Rotating disk electrode experiments, also, show that increase of power yield more active catalyst toward to oxygen reduction reaction. As a result, 25 W coating power is the optimum for the preparation of the smallest and the most active Pt particle in catalytic film.

© The Electrochemical Society of Japan, All rights reserved.

Keywords : Coating Parameters, Electrocatalysis, ORR, Sputtered Pt Filmsi

1. Introduction

Fuel cells have been receiving significant attention in the recent decades due to their high efficiency and environmental compatibility.[1] Among all fuel cell systems, proton exchange membrane fuel cells (PEMFCs) have shown a great promise as an alternative power sources, particularly for stationary power generation and transportation applications because of their low operating temperature, fast start-up, high power density, and low emission of pollutants.[2] Nevertheless the achieved substantial progress the PEMFCs are not broadly utilized since their cost and durability are still not satisfactory.

These are considered as the most serious impediments for the commercialisation of PEMFCs.[3] Platinum has been regarded as the most active catalyst both for the hydrogen oxidation reaction (HOR) and the oxygen reduction reaction (ORR). Much of the research on the PEMFCs is focused on improving the catalytic activity of the cathode electrocatalysts where the oxygen reduction reaction takes place, because ORR slow kinetics is responsible for about 70% of the total losses that occur in PEMFCs.[4–6]

The thin film deposition method of magnetron sputtering (MS) which is widely used for integrated circuit manufacturing, recently finds application as an alternative catalyst preparation and electrode assembling technique. The method is particularly favourable for applications in hydrogen energy converting electrochemical cells with polymer electrolyte membrane (PEM), including fuel cells, water electrolysers and unitized regenerative fuel cells. It allows deposition of thin compact films upon a selected substrate material and ensures simplicity of the catalysts preparation as well as improved stability, durability, and utilisation.[7–18] The sputter conditions are easily controlled in obtaining homogeneous, well dispersed and reproducible thin films of various single and composite materials with a very low loading. Using this method an essential decrease in the fuel cell cathode Pt loadings without reduction in performance has been already achieved.[7,11–14] It has been demonstrated that the sputter method insures very efficient usage and high mass activity of the platinum.[15–17] The technique was also applied for deposition of thin iridium oxide electyro-catalytic films as anode material for PEM water electrolysis and a 10 fold decrease of the catalyst loading has been reported compared to conventional iridium anodes.[18] On the other hand, how the sputter parameters effect the catalysts condition is still an enigma. It has been proven that sputter parameters such as dc or rf power, gas pressure, temperature, distance between the target and the substrate influence the not only film composition, but also its structure and morphology.

In a recently published paper, Huang et al.[9] have investigated the influence of rf power and argon partial pressure on the fuel cell performance, since they influence strongly the specific surface area and the electrochemical activity. The authors have observed that the rf power has much less effect on the properties of the sputtered Pt film than argon partial pressure. Wan et al.[19] have, also, studied the influence of low and high sputtering pressure on the deposition rate, porosity, and surface morphology and shorter deposition times at higher pressure value.

In the present paper, the catalytic efficiency and stability of thin sputter deposited Pt films, coated with different power, are investigated as catalyst for oxygen reduction reaction. The aim is to study the role of sputtering power on the electrochemically active surface area and the catalytic activity toward the oxygen reduction reaction in terms of exchange current density, j_o, as well as to access the catalytic performance characteristics at real operating conditions in a hydrogen PEMFC.

2. Experimental

A series of thin Pt films, the Pt loading is constant (22 $\mu g\,cm^{-2}$), were deposited by magnetron sputtering in argon plasma using a BesTec 222 UHV sputtering system. Pt targets with 6N grade purity are mounted on a two closed DC sputter gun, and loaded by Pt was run with 10, 15, 25, 50, 100 W. The sputtering chamber has a base pressure of 5×10^{-9} mbar and during the sputtering process (after feeding the chamber with Ar gas) it was between 1.4×10^{-3} and 1.5×10^{-3} mbar. The distance between metal targets and the substrate was set to 65 mm directly on a 5 cm^2 commercial hydrophobic carbon paper covered with a thin microporous film

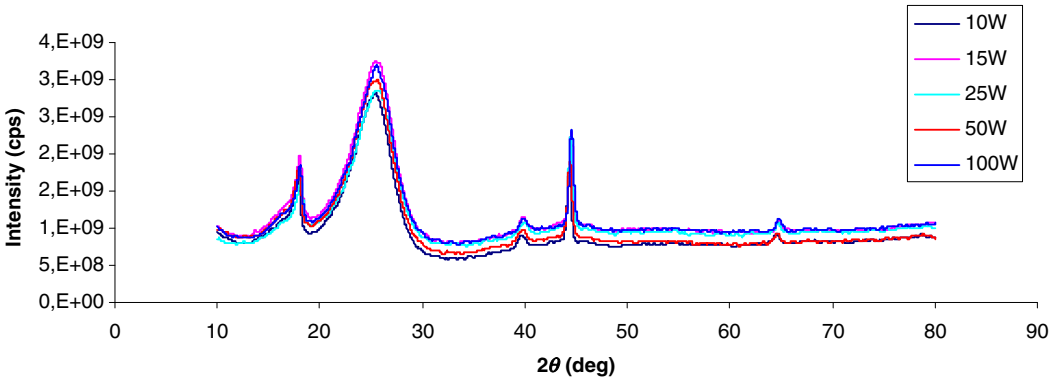


Figure 1. (Color online) XRD diffractograms of sputtered Pt layers.

of Vulcan-XC72 (*I3/C1*, Freudenberg) at room temperature. The carbon paper discs were positioned in precision-made stainless steel holders to exposure only their top surface to the sputtered flux. X-ray diffraction (XRD) analysis were performed on RIGAKU Smartlab, X-ray diffractometer using CuKα radiation (α = 1.54 Å). The XRD data were collected in the range of 10°–90° 2θ and continuous scan mode. SEM and EDX experiments were performed by a Philips XL 30 model scanning electron microscope (SEM).

During depositions, the platinum coverage were monitored by the quartz crystal microbalance (QCM) in conjunction with Ag $3d_{5/2}$ XPS as a function of Pt deposition. The parameters of QCM are calibrated by photoemission attenuations besides its default values. In order to determine the deposition ratios of the Pt film, the pure silver substrate is used to observe the attenuations of silver atoms photoemission as a function of additional material onto the substrate. For thickness determination using XPS signals both Ag $3d_{5/2}$ attenuation as a function of, as well as the Pt $4f_{7/2}$ to Ag $3d_{5/2}$ intensity ratio for a given films were compared.[3] In converting these ratios to films thickness, the electron mean free path was calculated by using the TPP formula developed by Tanuma, Powell, and Penn.[20]

The catalytic efficiency of the films toward ORR in 0.5 M H_2SO_4 solutions was investigated by means of cyclic voltametry (CV) and linear sweep voltametry (LSV) on rotating disc electrode (RDE), using Pine Instrument Bipotentiostat, model AFCBP1 controlled by PC and commercial software. The experiments were carried out in a three electrode electrochemical cell with Pt wire counter electrode and saturated Ag/AgCl reference electrode. All potentials in the paper were referred vs. RHE. In order to obtain reproducible data prior to ORR measurements the electrodes were electrochemically pre-treated by cycling the potential in the range −0.25 to 1.3 V for 50 cycles at scan rate of 100 mV s^{-1}. RDE polarization curves were recorded in oxygen saturated solution. The potential was swept in the range from −0.12 V to + 1.0 V (vs. RHE) at scan rate of 10 mV s^{-1}. The RDE polarisation curves were obtained at constant rotating speed 1600 rpm. The kinetic current density extracted from Koutecky Levich (K-L) plots was applied to construct the mass transfer corrected Tafel plots and to calculate the apparent exchange current density, j_o^{ap}, of the ORR.

Cyclic voltammograms in deaerated 0.5 M H_2SO_4 at 100 mV s^{-1} were recorded and used to assess the electrochemically active surface area, *EASA*, of the films via integration of the area under the hydrogen adsorption/desorption peaks.

3. Results and Discussion

The XRD patterns of the carbon-supported Pt coated with different powers are shown in Fig. 1. The diffraction peaks at ∼2θ = 18°, 24.6°, and 44.51° angles for all type of catalysts arise from the reflection of the support. All diffraction patterns display

Table 1. *EASA* ($m^2\ g_{Pt}^{-1}$), apparent exchange current density and exchange current density calculated from the cyclic voltammetry tests and linear sweep voltammetry.

Sputtering Power	*EASA*	J_o^{ap}	J_o	d (nm)
10	27.65	1.51×10^{-3}	5.46×10^{-8}	6.3
15	28.83	3.82×10^{-3}	1.32×10^{-7}	5.2
25	29.69	4.57×10^{-3}	1.53×10^{-7}	6.8
50	20.69	2.95×10^{-3}	1.42×10^{-7}	7.9
100	20.09	5.00×10^{-4}	2.48×10^{-8}	13.4

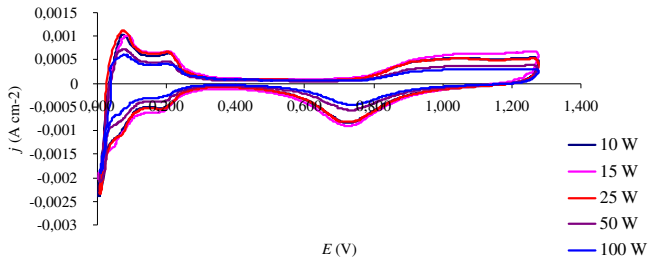


Figure 2. (Color online) Cyclic voltammograms of the test samples recorded in 0.5 M H_2SO_4 at 30°C; scan rate 100 mV s^{-1}.

the typical diffraction peaks (⟨111⟩, ⟨220⟩, and ⟨311⟩) of the fcc structure of platinum. Particle sizes of electrocatalyst were calculated from the broadening of (111) diffraction peak in XRD pattern of all catalysts by using Scherrer equation. Particle sizes of Pt are given in Table 1. It is seen that increasing of power does not change the particle size up to 25 W significantly. Otherwise, for 50 W and 100 W powers cause the bigger Pt particles.

The surface composition and the structure of the catalyst are the major parameters which affect its electrochemical performance. CV responses of the sputtered Pt films are presented in Fig. 2.

It can be seen that all CV curves have the shape of the pure Pt voltammogram which is well characterized in the literature,[21] implying that Pt atoms represent the main active sites for the redox reactions proceeding on the catalyst surface. Moreover, no anodic current that can be ascribed to the oxidation/dissolution except Pt, is demonstrating that the sputter magnetron is a clean process to prepare catalyst. Hydrogen adsorption/desorption region between 0.04 and 0.4 V vs. RHE is well depicted for all samples. The current peak associated with the reduction of oxygen is in the region above 0.8 V vs. RHE. The cyclic voltammograms are used to calculate the electrochemically active surface area of the electrodes under study, applying the well established procedure of integration the area under the hydrogen adsorption/desorption peaks and using the value of

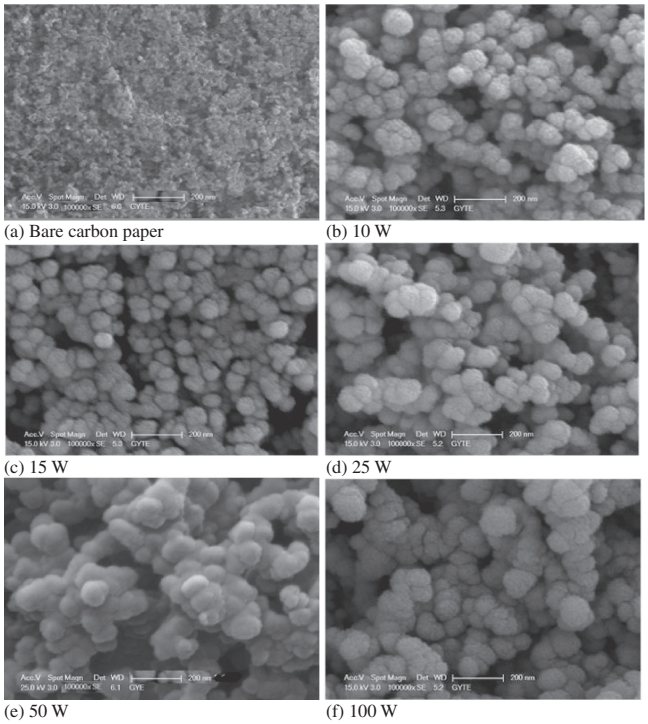


Figure 3. SEM images of the samples Bare Carbon Paper (a), 10 W (b), 15 W (c), 25 W (d), 50 W (e), 100 W (f).

210 μC cm^{-2} (the charge required for adsorption of hydrogen monolayer on 1 cm^2 of smooth Pt electrode) as a correction factor.[22]

The calculation shows that the *EASA* increases gradually with the increasing power, reaching a maximum of 29.69 m^2 g_{Pt}^{-1} for sample prepared with 25 W, but it was observed that further increase in sputtering power causes the decrease of electrochemical active surface area seriously. These observations clearly indicate that used power influences the film structure and morphology. Higher applied power results in higher acceleration of the ionized argon toward the target leading to sputtering of platinum particles with increased kinetic energy and longer mean free path. This reduces the probability of collisions with the Argon background gas. This higher kinetic energy leads to hit these Pt atoms or cluster the substrate surface with a higher probability for hopping events, lattice rearrangements, and surface remodelling. Those effects in turn, cause the formation of more densely packed of Pt atoms or clusters. This trend can be clearly seen from SEM images in Fig. 3. Rising the power from 10 W to 100 W Pt particles start to agglomeration and lost their *EASA*. The observed changes in the surface structure and morphology of the sputtered Pt films lead to essential variations in the electrochemically active surface area.

The electrocatalytic activity of the sputtered Pt films toward the oxygen reduction is assessed applying the method of linear sweep voltammetry and Koutecky–Levich plots based on Eq. (1). Figure 4 shows the RDE polarization curves for all catalysts under study.

The RDE polarization curves show characteristic behaviour reported in the literature for ORR on Pt in acid solutions with well distinguished regions of kinetic, mixed, and diffusion limited reaction rate. At very low overpotentials the process is governed by the charge transfer, then in the range down to 0.75–0.5 V the ORR reaction proceeds under mixed diffusion-kinetic control, after which the current starts to level out reaching diffusion limited values at potentials of 0.25–0.2 V.

The exchange current density, j_o, is a qualitative measure for the intrinsic activity of the catalyst. In order to calculate j_o, it is necessary first to construct the mass-transfer corrected Tafel slopes which in turn, requires determination of the kinetic current density.

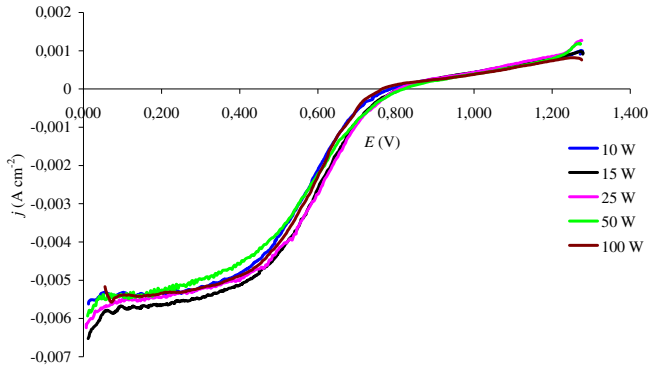


Figure 4. (Color online) RDE polarization curves in 0.5 M H_2SO_4 at 30°C; rotation rate 1600 rpm.

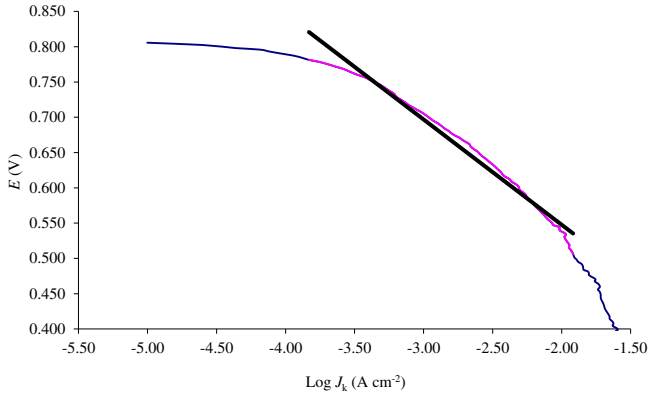


Figure 5. (Color online) Mass transfer corrected Tafel plots for the sample coated with 25 W.

One of the common approaches to calculate j_{kin}, is to solve Eq. (1) regarding the kinetic current at different potentials and given rotating speed. This relation is known as mass-transport correction for rotating disk electrodes.[4,23]

$$j_{kin} = \frac{j.j_{lim}}{j_{lim} - j} \quad (1)$$

Where j is the experimentally measured current density, $j_{lim.}$ - the measured diffusion-limited current density, and $j_{kin.}$ - the kinetic current density.

The obtained mass transfer corrected Tafel plot for sample coated with 25 W is presented in Fig. 5. Figure 5 shows a wide linear range (over 200 mV), which allows to determine the values of the Tafel slope and the apparent values of the exchange current density, j_o^{ap}. Since the apparent exchange current density does not reflect the true situation of ORR, hereafter all reference to exchange current density will be to the intrinsic exchange current density is to solve Eq. (2). All experimental results are summarized in Table 1.

$$j_o^{app} = (EASA).j_o.\left(\frac{P_{O_2}}{P^0{}_{O_2}}\right) \quad (2)$$

For all samples a single Tafel slope was obtained with a value close to 120 mV dec^{-1}, indicating the first electron transfer reaction as a rate determining step:

$$O_2 + e^- \rightarrow O^-{}_{2ads} \quad (3)$$

Usually, the presences of oxides on the Pt surface alter the kinetics of the ORR and yield a different Tafel slope.[24] Since this is obviously not the case for the sputtered deposited ultra thin Pt catalytic films, the observed promotion of the ORR must have another origin. The values of the exchange current density j_o in

Table 1 indicate a crucial increase in the intrinsic catalytic activity of Pt with rising power up to 25 W, but decrease with the increase of the power in consistent with the order of CV results. On the other hand, the polarization curves in Fig. 4 demonstrate that the oxygen reduction is most intensive for the 25 W sputtering powers, the catalyst that has the highest apparent exchange current density. The rate determining step and the ORR mechanism are identical on all power values. This means that the chemical rate constant and the potential dependent exponential terms are essentially the same, and the differences in the reaction kinetics must lie in the pre-exponential coverage-dependent term, which is determined by the OH^{-}_{ad} coverage. As expected, the increase of the sputtering power leads to an increase in *EASA* of the catalytic films and an improvement of the electrochemical activity toward ORR up to 25 W due to the increased number of active sites available. Therefore, the reactants can easily adsorb on the catalyst which intensifies the corresponding electrochemical reactions. On the other hand, at higher power than 25 W, both *EASA* and apparent current density decrease. The higher is the sputtering power the longer is the mean free path between the collisions of the sputtered particles with Ar atoms and radicals. This results in a higher kinetic energy when they reach the substrate. This higher energy makes the particles be capable to hop and rearrange thus, forming more dense metal film. Therefore, the optimum sputtering power was chosen as 25 W.

4. Conclusion

The research performed shows the possibilities to fabricate highly active and cost efficient Pt catalytic thin films with precisely controllable ultra low and homogeneous highly developed surface. It demonstrates that *EASA* increases gradually with the increasing power and reaching a maximum of $29.68\,m^2\,g_{pt}^{-1}$ for sample prepared with 25 W. On the other hand, further increases in power causes the decreases of *EASA* seriously. For all samples a single Tafel slope was obtained with a value close to $120\,mV\,dec^{-1}$ indicating the first electron transfer reaction as a rate determining step. It proves that a crucial increase in the intrinsic catalytic activity of Pt with rising power up to 25 W, but decrease with the increase of the power in consistent with the order of CV results. This is due to the increased number of active sites available for adsorption of the reactands on the catalysts. This same trend is clearly observed with SEM images. Rising power value causes the bigger catalyst particles and causes lower *EASA* and exchange current density. According to these results 25 W is the most effective dc power value for sputter magnetron coating technique.

References

1. Y. Saejeng and N. Tantavichet, *J. Appl. Electrochem.*, **39**, 123 (2009).
2. L. Jaeseung, S. Jungsook, H. Kookil, and K. Hasuck, *J. Power Sources*, **163**, 349 (2006).
3. O. Ozturk, O. K. Ozdemir, I. Ulusoy, A. S. Ahsen, and E. Slavcheva, *Int. J. Hydrogen Energy*, **35**, 4466 (2010).
4. H. A. Gasteiger, S. S. Kocha, B. Sompalli, and F. T. Wagner, *Appl. Catal., B*, **56**, 9 (2005).
5. H. A. Gasteiger, J. E. Panels, and S. G. Yan, *J. Power Sources*, **127**, 162 (2004).
6. J. H. Wee, K. Y. Lee, and S. H. Kim, *J. Power Sources*, **165**, 667 (2007).
7. A. T. Haug, R. E. White, J. W. Weidner, W. Huang, S. Shi, T. Stoner, and N. Rana, *J. Electrochem. Soc.*, **149**, A280 (2002).
8. M. Alvisi, G. Galtieri, L. Giorgi, R. Giorgi, E. Serra, and M. A. Signore, *Surf. Coat. Technol.*, **200**, 1325 (2005).
9. K. L. Huang, Y.-C. Lai, and C. H. Tsai, *J. Power Sources*, **156**, 224 (2006).
10. K. Makino, K. Furukawa, K. Okajima, and M. Sudoh, *J. Power Sources*, **166**, 30 (2007).
11. S. Y. Cha and W. M. Lee, *J. Electrochem. Soc.*, **146**, 4055 (1999).
12. S. Mukerjee, S. Srinivasan, and A. J. Appleby, *Electrochim. Acta*, **38**, 1661 (1993).
13. E. A. Ticianelli, J. G. Beery, and S. Srinivasan, *J. Appl. Electrochem.*, **21**, 597 (1991).
14. C. L. Chang, T. C. Chang, W. Y. Ho, J. J. Hwang, and D. Y. Wang, *Surf. Coat. Technol.*, **201**, 4442 (2006).
15. S. Hirano, J. Kim, and S. Srinivasan, *Electrochim. Acta*, **42**, 1587 (1997).
16. I. Radev, E. Slavcheva, and E. Budevski, *Int. J. Hydrogen Energy*, **32**, 872 (2007).
17. R. O'Hayre, S. J. Lee, S. W. Cha, and F. B. Prinz, *J. Power Sources*, **109**, 483 (2002).
18. D. Labou, E. Slavcheva, U. Schnakenberg, and S. Neophytides, *J. Power Sources*, **185**, 1073 (2008).
19. C. H. Wan, Q. H. Zhuang, C. H. Lin, M. T. Lin, and C. Shih, *J. Power Sources*, **162**, 41 (2006).
20. S. Tanuma, C. S. Powell, and D. R. Penn, *Surf. Sci.*, **192**, L849 (1987).
21. I. Avila-Garcia, M. Plata-Torres, M. A. Dominguez-Crespo, C. Ramirez-Rodriguez, and E. M. Arce-Estrada, *J. Alloys Compd.*, **434–435**, 764 (2007).
22. A. J. Bard and L. Faulkner, *Electrochemical Methods: Fundamentals and Applications*, John Wiley and Sons, New York, NY, p. 341 (2001).
23. M. D. Macia, J. M. Campina, E. Herrero, and J. M. Feliu, *J. Electroanal. Chem.*, **564**, 141 (2004).
24. A. Sarapuu, A. Kasikov, T. Laaksonen, K. Kontturi, and K. Tammeveski, *Electrochim. Acta*, **53**, 5873 (2008).